A Synergistic Coassembly of Block Copolymer and Fluorescent Probe in Thin Film for Fine-Tuning the Block Copolymer Morphology and Luminescence Property of the Probe Molecules

ARTICLE *in* MACROMOLECULES · DECEMBER 2012

Impact Factor: 5.8 · DOI: 10.1021/ma302041f

3 AUTHORS:

Biplab K. Kuila
Central University of Jharkhand
21 PUBLICATIONS **591** CITATIONS
SEE PROFILE

Chanchal Chakraborty
National Institute for Materials Science
20 PUBLICATIONS **95** CITATIONS
SEE PROFILE

Sudip Malik
Indian Association for the Cultivation of Science
68 PUBLICATIONS **1,051** CITATIONS
SEE PROFILE

Macromolecules

Article

pubs.acs.org/Macromolecules

A Synergistic Coassembly of Block Copolymer and Fluorescent Probe in Thin Film for Fine-Tuning the Block Copolymer Morphology and Luminescence Property of the Probe Molecules

Biplab K. Kuila,*[,†] Chanchal Chakraborty,[‡] and Sudip Malik*[,‡]

[†]Centre for Applied Chemistry, Central University of Jharkhand, Brambe, Ranchi 835205, India

[‡]Polymer Science Unit, Indian Association for the Cultivation of Science, 2A&2B Raja S. C. Mullick Road, Kolkata 700 032, India

Supporting Information

ABSTRACT: Here, we investigate a synergistic coassembly of a block copolymer, polystyrene-*b*-poly(4-vinylpyridine) (PS-*b*-P4VP), and a fluorescent probe molecule, pyrenebutyric acid (PBA), in thin film using block copolymer supramolecular assembly (SMA) strategy for a wide range of compositions tuned by varying the molar ratio (r) of PBA and 4VP units. The PBA molecules form supramolecules with PS-*b*-P4VP through H-bonding between the carboxylic acid group of 1-pyrenebutyric acid and pyridine ring of P4VP. For compositions r = 0, 0.1, 0.25, and 0.5, the SMAs exhibit cylindrical morphology, whereas for r = 0.75 and 1, the SMAs generate lamellar morphology. Interestingly, it has been observed that the orientation of the microdomains depends on the solvent used for annealing and can be switched reversibly on exposing the SMA films to corresponding solvent. In a nonselective solvent like chloroform, the microdomains are oriented normal to the substrate, whereas in a selective solvent like 1,4-dioxane, the microdomains are oriented parallel. The synergistic coassembly of PS-*b*-P4VP and PBA in SMAs with higher molar ratio results in a structure-within-structure pattern characterized by two length scales from phase separation of block copolymer and parallel $\pi-\pi$ stacking of the pyrene moiety of PBA molecules inside the comb block. The photophysical properties of PBA in different SMAs of varying composition were studied both in solution and in thin film state and compared to pure PBA. The UV−vis study shows the H type of aggregation of PBA molecules inside the comb block by parallel stacking of the pyrene units, and the PBA molecules orient parallel to the substrate when the microdomains are oriented normal to the substrate. The pure PBA molecules in thin film exhibit excimer emission extensively, whereas the PBA molecules in different supramolecular assemblies exhibit emission ranging from monomer to mixture of monomer and excimer. The SMA shows more intense fluorescence emission compared to pure PBA both in solution and in thin film.

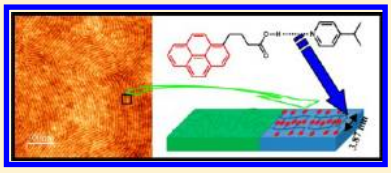

INTRODUCTION

Self-assembly of block copolymers (BCPs), in both bulk and thin film, has generated widespread research attention in the areas of nanoscience and nanotechnology due to their formation of fascinating set of periodic structures in the nanoscopic length scale.[1−4] The structural behavior of BCP thin films which is most important for its practical applications is often much more complicated compared to bulk materials due to the interfacial interactions of the blocks with the underlying substrate, the surface energies of the blocks, and commensurability of the film thickness. Controlling the orientation of microdomains and long-range order in BCP thin films is crucial, and significant progress has been made in this direction.[2−7]

In recent years, it has demonstrated that block copolymer supramolecular assembly where a low molar mass additive is associated with one of the blocks by noncovalent interactions[8−12] is a simple and powerful technique to introduce a new functionality into the block copolymer system as well as fine-tune its morphology. It has been successfully applied mainly in bulk[10,13−15] and in thin films[9,16−19] recently. The most commonly used block copolymers for such an approach are polystyrene-*block*-poly(4-vinylpyridine) (PS-*b*-PVP)[8,9,16,18,19] and polystyrene-*block*- poly(ethylene oxide) (PS-*b*-PEO).[20] The low-molecular-weight additives which have been extensively used are 3-pentadecylphenol (PDP),[8,19] dodecylbenzenesulfonic acid (DBSA),[8] and 2-(4′-hydroxybenzeneazo)benzoic acid (HABA).[16] Such supramolecular systems, which display a structure-within-structure pattern characterized by two length scales, have already been widely studied in bulk phase by Ikkala and ten Brinke.[13,21,22]

Recently, scientists are more interested in the study of block copolymer SMAs in thin film[15,17,23] because of their additional advantages over the block copolymer thin films.[9,16] Tung et al.[19] studied the effect of composition of PDP, interfacial interaction, and film thickness on the microscopic alignment of hierarchical assemblies of PS-*b*-P4VP (PDP) in thin films. A careful observation of AFM images reported on PS-*b*-P4VP (PDP) thin films indicated the huge surface roughness due to the unevenly distributed surfactant kind of additive (PDP) molecules over the thickness of the film, which limits their use for surface patterning application. The P4VP(PDP) either was

Received: September 27, 2012
Revised: December 4, 2012

   dx.doi.org/10.1021/ma302041f | *Macromolecules* XXXX, XXX, XXX−XXX

the matrix phase or formed one of the layers of lamellar structures. However, for nanotechnological applications it is important that the low-molecular-weight additive is present either in the cylindrical microdomains, which preferably should be oriented perpendicular to the substrate, or in spherical microdomains. This is because, in these structures, the removal of low-molecular-weight additive will lead to nanopores, which could then be used for nanopatterning applications. Nevertheless, it is possible to form cylindrical microdomains of P4VP(PDP) block either by adjusting the composition of the PS-*b*-P4VP block copolymer or by varying the PDP weight fraction in the SMA. However, the previous studies have shown that the obvious shortcoming in this case is that PDP being a surfactant preferably migrates to the surface, and hence the vertically oriented cylindrical microdomains of P4VP(PDP) block do not go through the complete film.[24]

Recently, Stamm et al. have demonstrated the synthesis of SMA from PS-*b*-P4VP and a small additive molecule 2-(4′-hydroxybenzeneazo)benzoic acid (HABA) where HABA selectively associated with the pyridine nitrogen via hydrogen bonding.[16] Thin films of SMA demonstrated well-ordered hexagonal cylindrical morphology where the cylindrical morphology was formed by P4VP(HABA) block surrounded by PS matrix.[16] The orientation of the cylindrical microdomains could be switched by exposure to different solvent vapors.[16a] After fabricating the order thin films from these supramolecular assemblies, the small molecules were removed from the thin film by selective dissolution and converted to nanoporous materials or nanotemplate.[9a,b,16a] These nanopores and nanochannels that are lined with functional groups have been used for further nanofabrications. Very recently, Sidorenko et al.[25] described novel block supramolecular assemblies in thin film, where the additive molecules selectively associate with one of the block by noncovalent interaction beyond hydrogen bonding.

The well-defined microphase separation of the block copolymers can also induce controlled and ordered assembly of the small additive molecules into nanoscopic length scale inside the block copolymer microdomains. So, block copolymer supramolecular strategies can be effectively used to tailor the physical properties (like optical, luminescence, electronic, etc.) of the functional small molecules by controlling their aggregation, as these properties highly depend on their nanostructured morphology.[26] The study of the structure properties relationship of these functional molecules is also very crucial for their applications in devices. Recently, Xu et al.[27] adopted quaterthiophene-based block copolymer supramolecular system to control the nanostructure of quaterthiophene and studied the field effect mobility of these supramolecular systems.

To date, most studies on the block copolymer supramolecular assemblies in thin film mainly concentrate on the phase separation of the block copolymer. There are very few reports where the individual assembly of the small molecules inside the block copolymer domain also been studied. The resultant functional properties of the small molecules due to their assembly in thin film are not much explored. In our previous article,[9a] we have reported the morphology of the assembly from block copolymer supramolecules containing PS-*b*-P4VP and PBA of single composition (4VP:PBA = 1:1) in thin film and their use for creating pattern of metal and semiconducting nanoparticle. In this article, we investigate the synergistic coassembly of polystyrene-*b*-poly(4-vinylpyridine) (PS-*b*-P4VP) and a fluorescent probe molecule, pyrenebutyric acid (PBA), in thin film using block copolymer supramolecular assembly (SMA) strategy for a wide range of compositions tuned by varying the molar ratio of PBA and 4VP unit. The PBA molecule is selectively chosen as it is an important fluorescent probe because of its valuable photophysical properties such as high fluorescence quantum yield, long fluorescence lifetime, high solvent polarity dependence of the vibrational structure of fluorescence spectra, and high ability for excimer formation and has been extensively used as sensors for the distinct fields of study.[28−31] The resultant synergistic coassemblies display a structure-within-structure pattern characterized by two length scales (one from phase separation of block copolymer and another due to the parallel stacking of the PBA molecules inside the comb block). The morphology of the block copolymer can be tuned from cylinder to lamella with different spacing and orientation depending on the composition of PBA and appropriate solvent annealing. The thin films generated from these hierarchical assemblies can be converted to porous template for further nanopatterning. The photophysical properties of PBA in supramolecular assemblies of varying composition were studied both in solution and in thin film state and also compared to pure PBA. It has been observed that the orientation of the PBA molecules with respect to substrate surface and their photophysical properties can be systematically and effectively controlled by block copolymer supramolecular assembly strategy. We believe that the study of these type of block copolymer supramolecular assembly thin films are not only interesting for their use for nanofabrication but also important for their potential applications such as luminescent sensing material.

EXPERIMENTAL SECTION

Materials. PS (32900)-*b*-P4VP (8000) (PDI = 1.06) was purchased from Polymer Source Inc. 1-Pyrenebutyric acid (PBA) (97%) was purchased from Sigma-Aldrich Chemicals and further purified by crystallization from ethanol. All the solvents used for experiments were purchased from Acros Organics and used as it is. Silicon wafers {100} were cleaned successively in an ultrasonic bath (dichloromethane) for 15 min and a "piranha" bath (30% H_2O_2, 70% of H_2SO_4, chemical hazard) for 90 min at 75 °C and then thoroughly rinsed with Millipore water and dried under an argon flow.

Sample Preparation. The characteristics of all the samples discussed in this paper are listed in Table 1. The diblock copolymer, PS-*b*-P4VP, and PBA of desired amounts were dissolved in 1,4-dioxane separately. PS-*b*-P4VP solution was then added drop-by-drop to PBA solution, while the solution was heated close to the boiling point of the solvent in an ultrasonic bath. The resulting solution (the total concentration PS-*b*-P4VP and PBA 1% (w/v)) was kept overnight to complete hydrogen-bonding formation. Thin films of PS-*b*-P4VP and PBA were prepared by the spin-coating method from the filtered composite solutions at spinning speed 2500 rpm. For UV−vis and

Table 1. Characteristics of PS-*b*-P4VP (PBA) SMA at Different PBA/4VP Molar Ratio

system	PBA/4VP(r)	$f_{P4VP(PBA)}$	f_{PBA}
SMA000	0.00	0.195	0.000
SMA001	0.01	0.200	0.005
SMA010	0.1	0.248	0.053
SMA025	0.25	0.290	0.118
SMA050	0.50	0.365	0.211
SMA075	0.75	0.425	0.286
SMA100	1.00	0.476	0.348

dx.doi.org/10.1021/ma302041f | *Macromolecules* XXXX, XXX, XXX−XXX

photoluminescence measurements, thin films from the composite solutions were deposited on clean quartz slide. The thickness of the polymer films on silicon substrate was measured by an SE 400 ellipsometer (SENTECH Instruments GmbH, Germany) with a 632.8 nm laser at a 70° incident angle. The thickness of the films was 30 ± 2 nm.

Solvent Vapor Annealing. The SMA thin films were further annealed in vapors of appropriate solvent for the reorientation of the microdomains and for improving the long-range order. The solvent vapor treatment of the thin films was done in a crystallographic dish with a Petri dish containing the solvent. The silicon substrate coated with the SMA film was kept in this crystallographic dish which then was completely closed. The sample was removed from the dish after a predetermined time during which the solvent in the film quickly evaporated. The annealing time was recorded from the moment when samples were put into or taken out from the crystallographic dish. All the samples used in this study were solvent vapor treated in the same crystallographic dish for the comparative experiments.

X-ray Study. WAXS experiments of the block copolymer supramolecular assemblies were performed on the bulk samples. Bulk samples were prepared by slowly evaporating the solvent from 1,4-dioxane solution of the supramolecular assembly taken in a Petri dish over 2 weeks. The experiments were carried out in a Seifert X-ray diffractometer (C 300) in reflection mode with a parallel beam optics attachment. The instrument was operated at a 35 kV and a 30 mA current and was calibrated with a standard silicon sample. Nickel-filtered copper Kλ radiation (λ = 0.154 nm) was used in the work. The samples were scanned from 2° to 15° at the step scan mode (step size 0.02°, preset time 2 s), and the diffraction pattern was recorded using a scintillation counter detector.

Atomic Force Microscopy. Atomic force microscopy (AFM) imaging was performed using a Dimension 3100 scanning force microscope (Digital Instruments, Inc., Santa Barbara, CA) and a CP microscope (Park Scientific Instrument, Inc.) in the tapping mode. The tip characteristics were spring constant 1.5−3.7 N m^{-1}, resonant frequency 45−65 Hz, and tip radius about 10 nm. Analysis of the AFM images was performed with the WSxM software (Nanotec Electronica).[32]

FTIR Study. Block copolymer thin films deposited on cleaned silicon wafers were directly used for FTIR measurements. Infrared spectra were recorded with a Nicolet FT-IR instrument [Magna-1R-750 spectrometer (series 11)].

UV−vis Study. UV−vis study of the SMA was done in both solution and thin film state. For the solution state measurement, 1% block copolymer supramolecular solutions in 1,4-dioxane were 1000 times diluted and taken in a quartz cell. In case of thin film measurement, the thin films of the supramolecular assemblies were deposited on quartz substrate by spin-coating. All the measurements were done using a UV−vis spectrometer (Hewlett-Packard, model 8453) at room temperature.

Photoluminescence Study. The photoluminescence (PL) measurement for the block copolymer supramolecules were done in both the solution and thin film state. For the solution state measurement, the block copolymer supramolecular solutions were prepared in 1,4-dioxane and taken the solution in a quartz cell of path length 1 cm. For the thin film measurements, the thin films of the supramolecular assemblies were deposited on quartz substrate by spin-coating. All the PL measurements were done in HORIBA Jobin Yvon (Fluoromax-3) luminescence spectrometer at room temperature. The photoexcitation was made at wavelength of 330 and 340 nm for solution and solid samples, respectively.

RESULTS AND DISCUSSION

The chemical structure of the block copolymer supramolecules based on PS-*b*-P4VP and PBA is shown in Figure 1. PBA associated with the P4VP block of PS-*b*-P4VP by hydrogen bonding, building comblike polymer chains. The block copolymer thin films based on supramolecular assembly of PS-*b*-P4VP and PBA were deposited on cleaned silicon wafer or

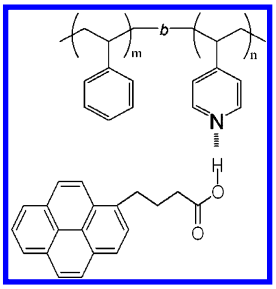

Figure 1. Chemical drawing of the SMA formation through hydrogen bonding between P4VP block of PS-*b*-P4VP copolymer and PBA.

quartz substrate by dip-coating from 1% composite solution in 1,4-dioxane. Table 1 lists different PS-*b*-P4VP (PBA)$_r$ (in which *r* denotes the ratio of PBA to the 4VP unit) supramolecules constructed varying the stoichiometries between the PBA and 4VP unit. The formation of comblike polymer chain through hydrogen bonding in different SMAs of varying PBA composition was investigated by FTIR study. Figure 2 (Figure 2a from 1030 to 980 cm^{-1} and Figure 2b from 1800 to 1620 cm^{-1}) shows the FT-IR spectra of PBA and different supramolecular assemblies. Free pyridine groups in the PS-*b*-P4VP (SMA000) contribute to the absorption at 994 cm^{-1} [14,19a] (which is absent in PBA spectra). After forming supramolecular assembly through hydrogen bonding, the absorption peak at 994 cm^{-1} becomes broad and its intensity decreases with increase in the concentration of PBA. In the case of supramolecular assemblies, a new broad peak appears at 1014 cm^{-1} which is due to the H-bonded pyridine ring.[9a,14,19a] The intensity of this absorption peak increases with increase in the concentration of PBA in different supramolecular assemblies which confirm the formation of hydrogen bonding between pyridine ring and PBA. The formation of hydrogen bonding is further confirmed by the band at 1695 cm^{-1}, which is corresponding to the stretching frequency of C═O bond from carboxylic acid group of PBA. As seen in Figure 2b, in the case of SMA001, SMA010, and SMA025, the peak at 1695 cm^{-1} become broader and trifurcated into three different peaks at 1673, 1705, and 1744 cm^{-1}. This trifurcation of the C═O stretching frequency in SMA001, SMA010, and SMA025 may be due to different types of arrangement of the pyrenebutyric acid inside the block copolymer microdomain which create different types chemical environment around the C═O bond.

When the concentration of PBA is lower, PBA can assemble in more different ways creating different arrangements of PBA inside the block copolymer domains. In the case of higher concentration (SMA050 and SMA100) of PBA the number of ways in which PBA can be arranged inside the block copolymer domain is limited. In case of SMA100 the PBA can arranged only in one way, resulting in a single arrangement of PBA molecules and one peak at 1709 cm^{-1}.

Microphase Separation in Thin Film. In this section we will discuss the microphase separation behavior of the supramolecular assemblies in thin film and how the solvent affects the orientation of the microdomains in thin film. All the AFM images discussed in this section were obtained from solvent annealed thin film after washing out PBA by dipping the thin film in ethanol. During washing the thin film by ethanol both surface reconstruction and the removal of PBA may occur together. Russell and co-workers[33] have shown such a surface reconstruction process in PS-*b*-P4VP diblock copolymer thin films and demonstrated that the preferential

dx.doi.org/10.1021/ma302041f | *Macromolecules* XXXX, XXX, XXX−XXX

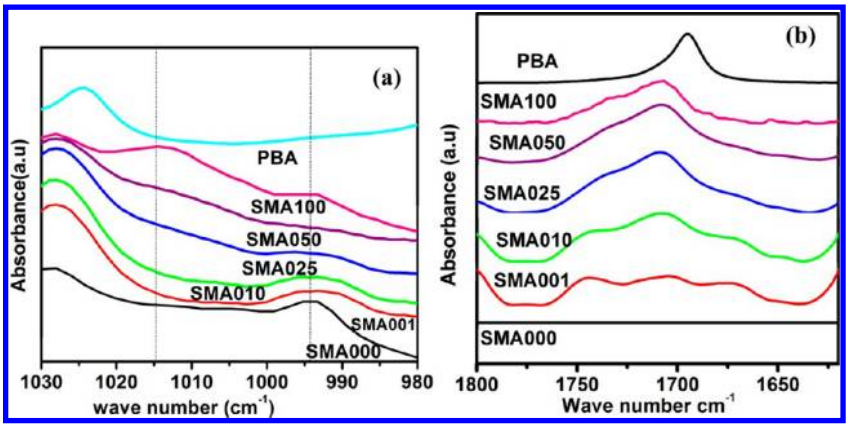

Figure 2. FT-IR spectra of PBA and different supramolecules in thin film in different regions: (a) 1030−980 cm^{-1}; (b) 1800−1620 cm^{-1}.

solvation of P4VP blocks with ethanol does not alter the order or orientation of the microdomains. At the same time, the PBA will be completely removed from the thin film due to high solubility of PBA in ethanol.[9a]

Figure 3 shows the AFM images of thin films casted from 1,4-dioxane and further annealed in 1,4-dioxane. The pure block copolymer (SMA000) used here exhibits hexagonally packed cylindrical channels oriented normal to the substrate.[9a] The AFM images of SMA010, SMA025, and SMA050 annealed in 1,4-dioxane vapor also show hexagonally packed cylindrical channels normal to the substrate. Such cylindrical vertical channels are created from the P4VP microdomain in case of SMA000 and P4VP(PBA) microdomain in the case of SMA001, SMA010, SMA025, and SMA050, after surface reconstruction or removal of PBA by dipping in ethanol. From the composition of the two blocks given in Table 1, cylindrical morphology is quite expected in SMA000, SMA010, SMA025, and SMA050, whereas the thin film of supramolecular assemblies SMA075 and SMA100 show lamellar morphology after being annealed in 1,4-dioxane, and the lamellar are oriented normal to the substrate as shown in the Figure 3e,f. Figure 4a−d shows the AFM height images of thin films of SMA casted from 1,4-dioxane solution and further annealed in chloroform vapor. The figure reveals parallel cylinder structures for SMA000, SMA010, SMA025, and SMA050, which are basically empty channels left after washing of PBA. Hence, the switching of microdomain orientation form perpendicular to parallel by changing annealing solvent from 1,4-dioxane to chloroform was observed for SMA000, SMA010, SMA025, and SMA050. The thin films of supramolecular assemblies from SMA075 and SMA100 were expected to give lamellar morphology with parallel orientation of the microdomains. Figure 4e,f shows the AFM height images of the thin films of SMA075 and SMA100 casted from 1,4-dioxane solution and annealed in chloroform after dipping in ethanol. Both the films reveal no characteristic regular morphology with uneven surface containing irregular channels which may be originated from parallel lamellar structure as these regular structures will be collapsed after dipping in ethanol. Table 2 indicates the interdomain spacing obtained from AFM height images for SMA samples annealed in 1,4-dioxane and chloroform. It is observed from Table 2 that the interdomain spacing increases with increase in the molar ratio of PBA in the SMAs as expected. Interestingly, it is observed for SMA010, SMA025, and SMA050 that the interdomain spacing of the samples annealed in chloroform is larger than those annealed in 1,4-dioxane. The larger interdomain spacing in chloroform is attributed to the distortion of the hexagonal lattice after drying of the film swollen in chloroform vapors.[16b]

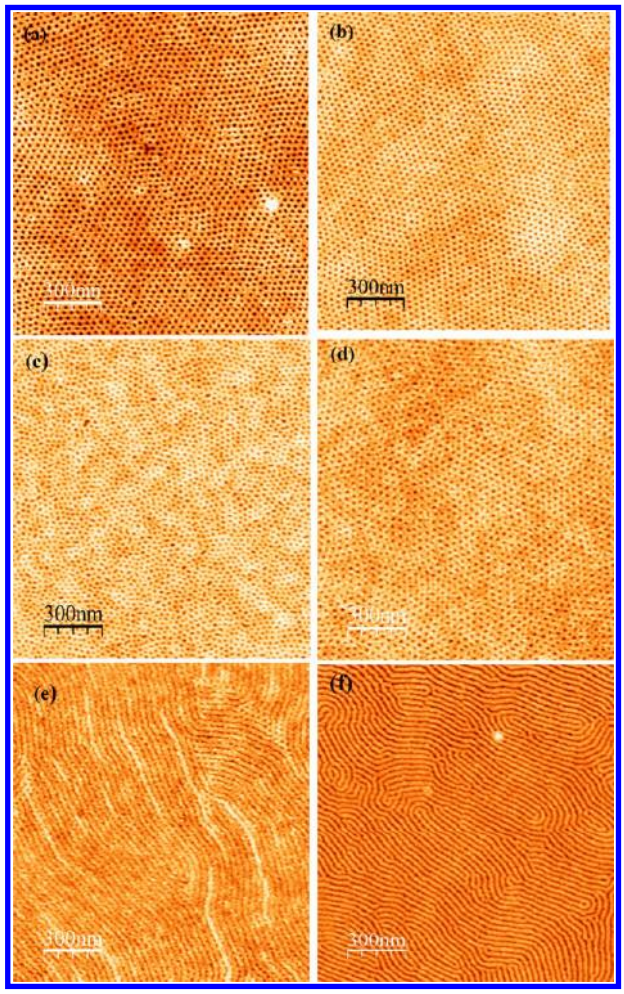

Figure 3. AFM height images of the thin film casted from 1,4-dioxane solution. The thin films are further annealed in 1,4-dioxane vapors and surface reconstructed (a) SMA000, (b) SMA010, (c) SMA025, (d) SMA050, (e) SMA075, and (f) SMA100.

The similar preferential orientation and switching of the microdomains (parallel or normal to the substrate) depending on different solvent used for annealing is also supported by other literatures.[16,34] Sidorenko et al.[16a] demonstrated the

dx.doi.org/10.1021/ma302041f | Macromolecules XXXX, XXX, XXX−XXX

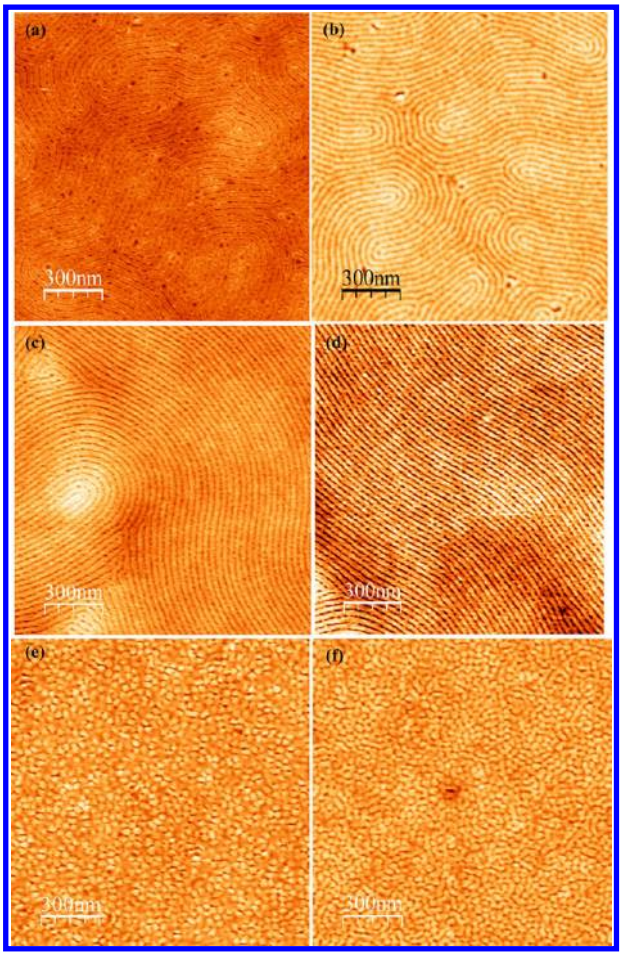

Figure 4. AFM height images of the thin film casted from 1,4-dioxane solution. The thin films are further annealed in chloroform vapors and surface reconstructed (a) SMA000, (b) SMA010, (c) SMA025, (d) SMA050, (e) SMA075, and (f) SMA100.

Table 2. Interdomain Spacing of Different Supramolecular Assemblies at Different PBA/4VP Molar Ratios in Thin Films

	thin film morphology at 25 °C		domain spacing (nm)	
system	1,4-dioxane	chloroform	1,4-dioxane	chloroform
SMA000	⊥ cylinder	∥ cylinder	26.12	28.3
SMA010	⊥ cylinder	∥ cylinder	26.21	28.5
SMA025	⊥ cylinder	∥ cylinder	26.7	28.9
SMA050	⊥ cylinder	∥ cylinder	27.5	29.3
SMA075	⊥ lamella	∥ lamella	28.2	
SMA100	⊥ lamella	∥ lamella	29	

reversible switching phenomenon in a supramolecular assembly upon exposure to different solvent in thin film. We have used such switching phenomenon to determine the morphology of different compositions of the PS-*b*-P4VP and PBA supramolecular system in two different solvents, 1,4-dioxane and chloroform. The preferential orientations of the microdomains can be attributed to the selectivity of the constituted blocks in that solvent used for solution preparation and annealing. 1,4-Dioxane is a selective solvent for PS not for P4VP or P4VP (PBA) block. So annealing in 1,4-dioxane will induce the morphology that consists of microdomains normal to the substrate. The morphology obtained upon evaporation of 1,4-dioxane is a metastable morphology and annealing in a nonselective solvent leads to an equilibrium morphology where the microdomains are parallel to the substrate. Here the chloroform which is a nonselective solvent for the block copolymer leads to orientation of the microdomains parallel to the substrate. The mechanism of such switching has been discussed in the literature, and the transformation from perpendicular to parallel domain orientation in chloroform involves domain breakup, induced by thermodynamically unstable interface, and then coalescence of the domains along the plane of the film.[34]

The microphase separation of the pure block copolymer and SMA100 in thin film was investigated by a GISAX study in our previous paper.[9a] The pure block copolymer in thin film shows hexagonally packed cylindrical morphology with periodicity of 26 nm whereas the SMA with 4VP:PBA (1:1 molar ratio) shows lamellar morphology with periodicity 29 nm, and the orientation of the microdomains is normal to the substrate. In order to investigate the ordering and the spatial arrangement of the PBA inside the block copolymer domain, WAXS experiment was performed on the bulk sample. Figure 5a shows the

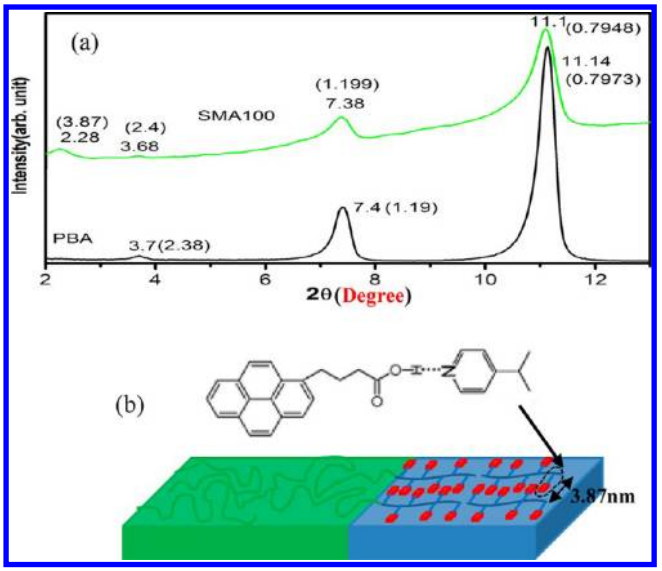

Figure 5. (a) WAXS patterns of PBA and SMA100; the 2θ value corresponding to each peak is shown in the figure, whereas the corresponding d spacing in nm is shown in parentheses. (b) Schematic diagram of the arrangement of the block copolymer chains and PBA molecule.

WAXS patterns of pure PBA and SMA100. The pure pyrenebutyric acid has highly ordered lamellar structure with 2θ values of 3.7°, 7.4°, and 11.14° corresponding to d-spacing of 2.38 nm (001 reflection), 1.19 nm (002 reflection), and 0.794 nm (002 reflection), respectively.[35] In SMA100, the peaks from the crystal of pure PBA are 3.68°, 7.38°, and 11.1°, which correspond to the d spacing of 2.4, 1.199, and 0.7948 nm, respectively. The slight change in d spacing in SMA100 may be due to the different type of aggregation of the PBA molecules in the crystal as discussed in the UV−vis study. In SMA100 there appears an additional peak at lower angle 2θ = 2.28°, which corresponds to a lamella spacing of 3.87 nm due to the order arrangement of the PBA molecules inside the block copolymer domains as depicted in Figure 5b. Assuming similar phase behavior both in bulk and in thin film, the WAXS patterns of the supramolecular assembly SMA100 confirm a

dx.doi.org/10.1021/ma302041f | *Macromolecules* XXXX, XXX, XXX−XXX

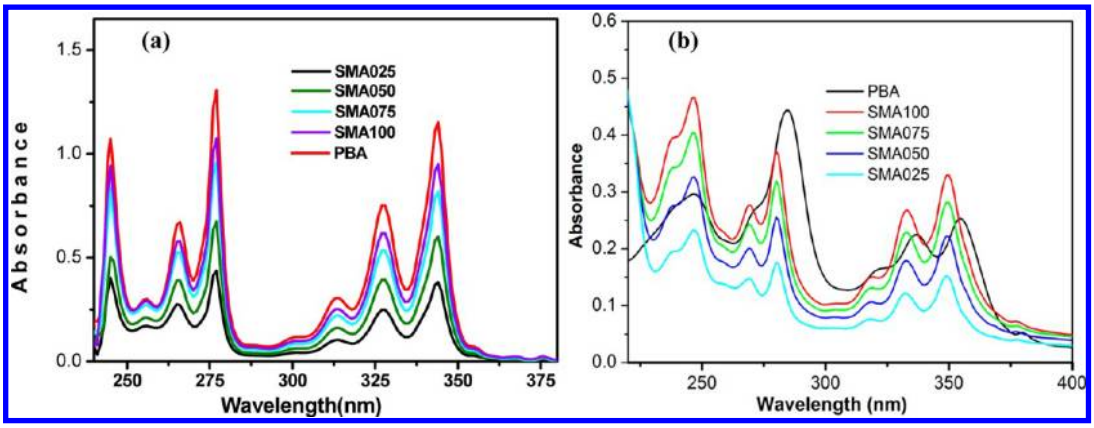

Figure 6. UV−vis spectra of PBA and different supramolecular assemblies containing varying composition of PBA (a) in solution of 1,4-dioxane and (b) in thin film state.

lamellae-within-lamellae hierarchical assembly where the block copolymer forms a lamellar morphology with a periodicity of 29 nm and the P4VP(PBA) comb block forms lamellae with a periodicity of ∼3.87 nm. As in this case, the block copolymer microdomains are oriented normal to the substrate, the probable orientation of the PBA molecules will be parallel to the surface of the substrate as depicted in Figure 5b. Such type of hierarchical assembly by synergistic coassembly of PS-*b*-P4VP and additive molecules in bulk phase is well investigated in earlier literature[17,21,22] and recently reported in thin films.[19] The molecules used in SMA showing hierarchical structure generally have a long alkyl chain to crystallize. In this SMA system, the parallel $\pi-\pi$ stacking of the pyrene moiety of PBA molecules stabilizes synergistically the periodic nanostructures created by the PBA molecules. A similar type of periodic lamellar structure from an organic−inorganic hybrid of zinc oxide and pyrenebutyric acid was reported by Stupp et al.[36] where the $\pi-\pi$ interaction stabilizes the periodic nanostructure.

UV−vis Study. UV−vis absorption spectra of pure PBA and the supramolecules in 1,4-dioxane are shown in Figure 6. In the solution state, PBA shows absorption peaks (Figure 6a) at 245, 256, 266, 277, 300, 313, 327, and 344 nm. The absorption peaks of PBA in different supramolecular assemblies in 1,4-dioxane dilute solution do not produce any significant change compared to pure PBA. The absorbance of PBA decreases with decrease of the concentration of PBA in different SMAs. Figure 6b shows the UV−vis absorption spectra of PBA and different SMAs in thin film state. Pure PBA shows absorption peak at 247, 271, 322, 284, 337, 355, and 380 nm, whereas the supramolecules at 247, 269, 280, 318, 333, 350, and 377 nm. As shown from the Figure 6b, in all the supramolecular assemblies, the UV−vis absorption peaks of PBA at 247 nm remain unchanged, but the peaks at 271, 284, 322, 337, 355, and 380 nm are blue-shifted to 269, 280, 318, 333, 350, and 377 nm, respectively. The pure PBA shows absorption peak with λ_{max} at 271, 284, 322, 337, 355, and 380 nm are due to the $\pi-\pi^*$ transition moment of the planar pyrene unit.[37,38] In case of supramolecular assembly the blue shift is due to different type of aggregation of the PBA molecules, probably H-type of aggregation, compared to the pure PBA.

The H-type of aggregation of PBA molecules is highly possible as the microphase separation of the block copolymer will induce parallel stacking of the pyrene units resulting H type of aggregation. The pyrene moiety has two electronic transition moments; the moment for the first band (A_{284}, λ = 284 nm) is known to be perpendicular to the molecular axis, and the second band (A_{355}, λ = 355 nm) has a transition moment parallel to it.[37a] These transition moments lie in the plane of the chromophore. The orientation of the PBA molecules can be evaluated from the ratio of the integrated peak area calculated from curve fitting and deconvolution method.[38] The integrated peak areas of these two absorption bands whose λ_{max} at 284 and 355 nm respectively for pure PBA and different supramolecular assemblies are summarized in Table 3. Since $area_{284}/area_{355}$ for different supramolecular assemblies are smaller (with increase of the PBA stoichiometry, $area_{284}/area_{355}$ values decreases, Table 3) than that for pure PBA thin film, the PBA molecules must orient parallel to the layer plane in all these supramolecular assemblies, whereas the pure PBA molecules in thin film will orient perpendicular to the layer plane. The parallel arrangement of the PBA molecules is supported by X-ray study as discussed earlier.

Table 3. UV−vis Absorbance of Different Supramolecular Assemblies at λ = 284 and 355 nm (Summarized from Figure 6b)

system	$area_{284}$	$area_{355}$	$area_{284}/area_{355}$
PBA	5.62	2.043	2.75
SMA025	0.48	1.299	0.36
SMA050	0.75	2.364	0.31
SMA075	0.923	3.232	0.29
SMA100	1.153	4.004	0.28

Photoluminescence (PL) Spectra. Steady-state PL was recorded after exciting the composite and the pure PBA in 1,4-dioxane solution at wavelength of 330 and 340 nm for solution and solid samples, respectively. Figure 7 shows the PL spectra of the pure PBA and the composites both in solution in 1,4-dioxane (Figure 7a) and thin film state (Figure 7b). The monomer and excimer emissions of all the compositions are summarized in Table 4. As shown from the Figure 7a, the pure PBA solution shows strong broad and structureless emission peak from 400 to 600 nm. This emission peak is due to the excimer formation from the aggregation of PBA molecules in 1,4-dioxane at this high concentration of PBA (3×10^{-3} mol/L). SMA001 emits almost pure monomer emission (showing few peaks and the fine structures in the range 370−410 nm) with almost no excimer emission (broad peak from 420 to 550 nm), whereas the supramolecular assemblies with other composition show both monomer and excimer emission

dx.doi.org/10.1021/ma302041f | *Macromolecules* XXXX, XXX, XXX−XXX

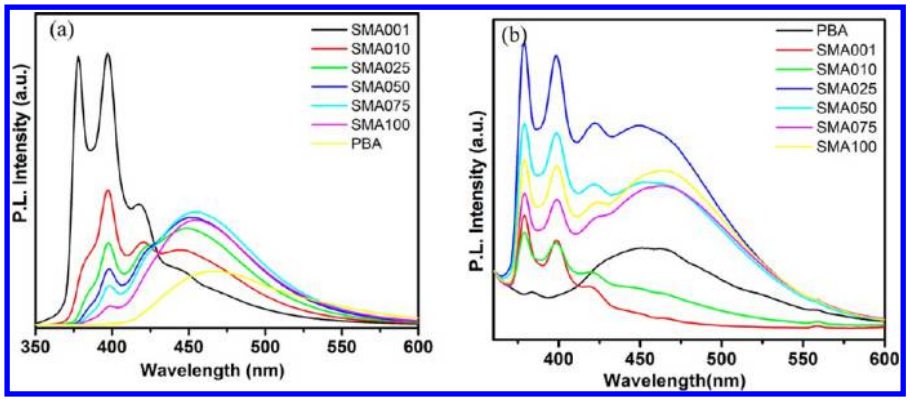

Figure 7. PL spectra of PBA and different supramolecular assemblies containing varying composition of PBA (a) in solution of 1,4-dioxane and (b) in thin film state.

Table 4. Key Photophysical Data of PBA and Different Supramolecular Assemblies (Summarized from Figure 7)

composition	I_E/I_M in solution state	I_E/I_M in solid state	I_{379}/I_{399} in solid state	I_{379}/I_{399} in solution state
PBA		1.91		
SMA001	0.1956	0.169	1.249	0.987
SMA010	0.5531	0.429	1.109	
SMA025	1.179	0.720	1.045	
SMA050	1.92	0.728	1.045	
SMA075	2.899	0.9568	1.045	
SMA100	5.652	0.9423	1.030	

bands. In the case of supramolecular assemblies the excimer emission could be attributed to the excimer formation by parallel stacking of the pyrene moiety of PBA in a single P4VP chain. The more the PBA stoichiometry increases, the more the ratio of the excimer and monomer emission (I_E/I_M) is enhanced (Table 4). The excimer emission peaks of the composite solution are blue-shifted and less broad compared to pure PBA. The blue shift of the emission peak in case of SMAs is probably due to H-type of aggregation of the PBA molecules in solution under the influence of block copolymer compared to pure PBA. The less broadening of the excimer emission peak is due to the more regular aggregation of the PBA molecules inside the block copolymer domain.[37] In the case of SMA100 the intensity of the excimer emission peak is less than the intensity of the excimer emission of SMA075 although the former has a higher concentration of PBA than the latter.

Figure 7b shows the PL spectra of the thin films of PBA and the SMAs with different composition of PBA. In thin film state PBA generates a broad excimer peak with a very little monomer emission. The SMA with low PBA content (SMA001 and SMA010) produces almost pure monomer emission whereas other SMA with higher PBA content shows both monomer and excimer emission. In the lower concentration of PBA, each PBA molecule will be isolated by supramolecular assembly with the P4VP chain, and the pyrene residue will be less accessible to each other and unable to form excimer (Figure 8). Whereas, in the SMA with higher PBA content, the pyrene moiety of PBA molecule will be more accessible to each other by parallel stacking inside the block copolymer microdomain. The SMA025 provides the highest monomer and excimer emission although it has lesser PBA content than SMA050, SMA075, and SMA100. In case of SMA025, SMA050, and SMA075, the monomer emission intensities decrease with increasing PBA concentration, whereas in the case of SMA100 again the

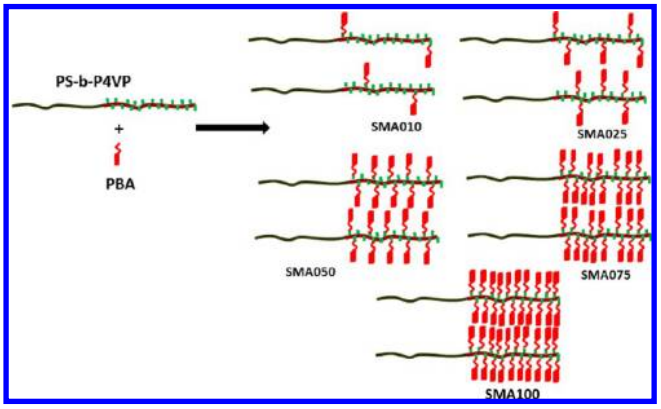

Figure 8. Possible arrangement of the PBA molecules in different supramolecular assemblies depending on composition of PBA.

monomer emission intensity increases. One of the important observations is that PBA in thin film show almost excimer emission, whereas after supramolecular assembly the emission properties of pristine PBA is modified. In the case of SMA001 and SMA010, only monomer emission is observed, whereas both monomer and excimer emission are observed in the case of SMA025, SMA050, SMA075, and SMA100. The emission intensity of both monomer and excimer is also increased after forming supramolecular assembly. The increase in the intensity of the monomer and excimer emission in the case of SMA with lower content of PBA may be due to the isolation of PBA molecules from each other which prevent quenching of emission from nonradiative decay due to intermolecular interaction. Also more regular assembly of the PBA molecules inside the block copolymer domain attributes less quenching of emission caused by nonradiative decay compared to pure PBA thin film. With increasing PBA content in different SMA, the ratio of intensity of excimer to monomer emission (I_E/I_M) increases (Table 4). If we compare I_E/I_M of SMAs in solution and solid phase, the values of I_E/I_M are higher in the case of solution phase compared to solid phase. It suggests that the molecular motion of the pyrene probe is also restricted in the thin film state. It has been reported that the intensity ratio I_{379}/I_{399} is often utilized to investigate the polarity of the surrounding molecular environment.[37] The value of I_{379}/I_{399} increases with increase of the environmental polarity (Table 4). In the case of solution state, we have observed that, except for SMA001, all other SMAs do not show a well-defined emission peak at 379 nm, which may be due to strong excimer emission

dx.doi.org/10.1021/ma302041f | *Macromolecules* XXXX, XXX, XXX−XXX

which affects the band of monomer emission and due to relatively low solvent polarity of 1,4-dioxane used in solution preparation. In the case of thin film state, it is interesting to observe that the value of I_{379}/I_{399} decreases from SMA001 to SMA010, whereas it is constant for SMA025, SMA050, and SMA075 and again decreases to SMA100. This confirms that in different supramolecular assembly the pyrene moieties of PBA are in different molecular environment, which is expected from the different type of packing of PBA molecules inside the block copolymer domain depending on the stoichiometric ratio of PBA/4VP. As more and more PBA molecules are packed into the comb block, the polarity is decreased and hence I_{379}/I_{399} decreases. The change in the fluorescence property of PBA after supramolecular assembly can also be identified visibly (Supporting Information, Figure S1). PBA emits a pale blue color from monomer emission, and emits a yellow-green color from excimer emission. The SMA001 and SMA010 thin films show a pale blue color, the intensity of pale blue color decreases with increase in PBA concentration, and pure PBA thin film turns almost yellow-green under UV light illumination (λ = 365 nm).

CONCLUSION

In conclusion, we have described the phase behavior of a block copolymer supramolecular assembly (SMA) consisting of a fluorescent probe molecule pyrenebutyric acid (PBA) of wide range of compositions tuned by varying the molar ratio (r) of PBA and 4VP unit in thin film. The supramolecular assemblies with molar ratio of (r = 1) display a structure-within-structure pattern characterized by two length scales, i.e., ∼29 and ∼3.87 nm, simultaneously from phase separation of block copolymer and parallel $\pi-\pi$ stacking of the pyrene moiety of PBA molecules inside the comb block. The block copolymer morphology and the aggregation of PBA inside the comb block are simultaneously tuned by changing the stoichiometry of PBA in the SMAs. The SMA thin films show cylindrical or lamellar morphology depending on the composition. For compositions r = 0, 0.1, 0.25, and 0.5, the SMAs exhibit cylindrical morphology, whereas for r = 0.75 and 1, the SMAs exhibit lamellar morphology. The orientation of the microdomains can be reversibly switched on exposing the SMA film with appropriate solvent. In a nonselective solvent like chloroform, the microdomains are oriented normal to the substrate, whereas in a selective solvent like 1,4-dioxane the microdomains are oriented parallel. The UV−vis study shows the H-type of aggregation PBA molecules inside the comb block by parallel stacking of the pyrene units of PBA molecules, and the PBA molecules orient parallel to the substrate when the microdomains are oriented normal to the substrate. The pure PBA molecules in thin film exhibit excimer emission extensively, whereas the PBA molecules in different supramolecular assemblies exhibit emission ranging from monomer to mixture of monomer and excimer. The SMA shows more intense fluorescence emission compared to pure PBA both in solution and in thin film. This study suggests that the molecular orientation of the luminescent molecules is efficiently controlled in thin film by block copolymer supramolecular assembly. The study of these types of block copolymer supramolecular assembly thin films is not only interested for their use for nanofabrication but also may be important for their potential applications such as luminescent sensing material.

ASSOCIATED CONTENT

Supporting Information

Figure S1. This material is available free of charge via the Internet at http://pubs.acs.org.

AUTHOR INFORMATION

Corresponding Author

*E-mail biplab.kuila@yahoo.com (B.K.P.), psusm2@iacs.res.in (S.M.).

Notes

The authors declare no competing financial interest.

ACKNOWLEDGMENTS

Dr. Biplab K. Kuila acknowledges Department of Science and Technology, Government of India, for financial support under Ramanujan Fellowship (SR/S2/RJN-81/2010). C.C. is indebted to CSIR, New Delhi, Govt. of India. Authors also acknowledge Dr. K. Dana of CSIR-CGCRI, Kolkata for helping in curve fitting and deconvolution.

REFERENCES

(1) (a) Hamely, I. W. *The Physics of Block Copolymers*; Oxford University Press: New York, 1998. (b) Bates, F. S.; Fredrickson, G. H. *Annu. Rev. Phys. Chem.* **1990**, *41*, 525. (c) Bates, F. S.; Fredrickson, G. H. *Phys. Today* **1999**, *52*, 32.

(2) (a) Darling, S. B. *Prog. Polym. Sci.* **2007**, *32*, 1152. (b) Ramanathan, M.; Nettleton, E.; Darling, S. B. *Thin Solid Films* **2009**, *517*, 4474. (c) Knoll, A.; Horvat, A.; Lyakhova, K. S.; Krausch, G.; Sevink, G. J. A.; Zvelindovsky, A. V.; Magerle, R. *Phys. Rev. Lett.* **2002**, *89*, 035501.

(3) Chen, J. T.; Thomas, E. L.; Ober, C. K.; Mao, G. P. *Science* **1996**, *272*, 343.

(4) Thurn-Albrecht, T.; Schotter, J.; Kastle, G. A.; Emley, N.; Shibauchi, T.; Krusin-Elbaum, L.; Guarini, K.; Black, C. T.; Tuominen, M. T.; Russell, T. P. *Science* **2000**, *290*, 2126.

(5) Segalman, R. A. *Mater. Sci. Eng. R* **2005**, *48*, 191.

(6) Hawker, C. J.; Russell, T. P. *MRS Bull.* **2005**, *30*, 952.

(7) Morkved, T. L.; Lu, M.; Urbas, A. M.; Ehrichs, E. E.; Jaeger, H. M.; Mansky, P.; Russell, T. P. *Science* **1996**, *16*, 931.

(8) Ikkala, O.; ten Brinke, G. *Chem. Commun.* **2004**, 2131.

(9) (a) Kuila, B. K.; Gowd, E. B.; Stamm, M. *Macromolecules* **2010**, *43*, 7713. (b) Kuila, B. K.; Nandan, B.; Bohme, M.; Janke, A.; Stamm, M. *Chem. Commun.* **2009**, 5749. (c) Kuila, B. K.; Stamm, M. *J. Mater. Chem.* **2010**, *20*, 6086. (c) Nandan, B.; Kuila, B. K.; Stamm, M. *Eur. Polym. J.* **2011**, *47*, 584. (d) Kuila, B. K.; Stamm, M. *J. Mater. Chem.* **2011**, *21*, 141271. (e) Kuila, B. K.; Rama, M. S.; Stamm, M. *Adv. Mater.* **2011**, *23*, 1797. (f) Kuila, B. K.; Stamm, M. *Macromol. Rapid Commun.* **2010**, *31*, 1881.

(10) Wood, K. C.; Little, S. R.; Langer, R.; Hammond, P. T. *Angew. Chem., Int. Ed.* **2005**, *44*, 6704.

(11) Faul, C. F. J.; Antonietti, M. *Adv. Mater.* **2003**, *15*, 673.

(12) Thunemann, A. F. *Prog. Polym. Sci.* **2002**, *27*, 1473.

(13) Valkama, S.; Ruotsalainen, T.; Nykanen, A.; Laiho, A.; Kosonen, H.; ten Brinke, G.; Ikkala, O.; Ruokolainen, J. *Macromolecules* **2006**, *39*, 9327.

(14) Ruokolainen, J.; Saariaho, M.; Ikkala, O.; ten Brinke, G.; Thomas, E. L.; Torkkeli, M.; Serimaa, R. *Macromolecules* **1999**, *32*, 1152.

(15) Osuji, C. O.; Chao, C. Y.; Ober, C. K.; Thomas, E. L. *Macromolecules* **2006**, *39*, 3114.

(16) (a) Sidorenko, A.; Tokarev, I.; Minko, S.; Stamm, M. *J. Am. Chem. Soc.* **2003**, *125*, 12211. (b) Tokarev, I.; Krenek, R.; Burkov, Y.; Schmeisser, D.; Sidorenko, A.; Minko, S.; Stamm, M. *Macromolecules* **2005**, *38*, 507.

(17) van Zoelen, W.; Asumaa, T.; Ruokolainen, J.; Ikkala, O.; ten Brinke, G. *Macromolecules* **2008**, *41*, 3199.

(18) (a) Laforgue, A.; Bazuin, C. G.; Prudhomme, R. E. *Macromolecules* **2006**, *39*, 6473. (b) Tang, C.; Lennon, E. M.; Fredrickson, G. H.; Kramer, E. J.; Hawker, C. J. *Science* **2008**, *322*, 429.
(19) (a) Tung, S.-H.; Kalarickal, N. C.; Mays, J. W.; Xu, T. *Macromolecules* **2008**, *41*, 6453. (b) Tung, S.-H.; Xu, T. *Macromolecules* **2009**, *42*, 5761. (c) Kao, J.; Tingsanchali; Xu, T. *Macromolecules* **2011**, *44*, 4392.
(20) (a) Morikawa, Y.; Nagano, S.; Watanabe, K.; Kamata, K.; Iyoda, T.; Seki, T. *Adv. Mater.* **2006**, *18*, 883. (b) Cheyne, R. B.; Moffitt, M. G. *Langmuir* **2006**, *22*, 8387. (c) Cha, M.-A.; Shin, C.; Kannaiyan, D.; Jang, Y. H.; Kochuveedu, S. T.; Ryu, D. Y.; Kim, D. H. *J. Mater. Chem.* **2009**, *19*, 7245.
(21) Ruokolainen, J.; Makinen, R.; Torkkeli, M.; Makela, T.; Serimaa, R.; ten Brike, G.; Ikkala, O. *Science* **1998**, *280*, 557.
(22) Ikkala, O.; ten Brinke, G. *Science* **2002**, *295*, 2407.
(23) Albrecht, K.; Mourran., A.; Zhu, X.; Markkula, T.; Groll, J.; Beginn, U.; deJeu, W. H.; Moeller, M. *Macromolecules* **2008**, *41*, 1728.
(24) Tokarev, I. PhD Dissertation, Technische University at Dresden, 2005.
(25) Hagaman, D.; Enright, T. P.; Sidorenko, A. *Macromolecules* **2012**, *45*, 275.
(26) (a) Yu, G.; Gao, J.; Hummelen, J. C.; Wudl, F.; Heeger, A. J. *Science* **1995**, *270*, 1789. (b) Greenham, N. C.; Moratti, S. C.; Bradley, D. D. C.; Friend, R. H.; Holmes, A. B. *Nature* **1993**, *365*, 628. (c) Nelson, J. *Science* **2001**, *293*, 1059. (d) Coakley, K. M.; McGehee, M. D. *Chem. Mater.* **2004**, *16*, 4533. (e) Brabec, C. J.; Sariciftci, N. S.; Hummelen, J. C. *Adv. Funct. Mater.* **2001**, *11*, 15.
(27) Rancatore, B. J.; Mauldin, C. E.; Tung, S.-H.; Wang, C.; Hexemer, A.; Strzalka, J.; Frechet, J. M.; Xu., T. *ACS Nano* **2010**, *4*, 2721.
(28) Birks, J. B. *Photophysics of Aromatic Molecules*; Wiley-Interscience: New York, 1970; Chapter 7.
(29) Kalyanasundaram, K.; Thomas, J. K. *J. Am. Chem. Soc.* **1977**, *99*, 2039.
(30) Deumie, M.; Baraka, M. E.; Quinones, E. *J. Photochem. Photobiol. A: Chem.* **1995**, *87*, 105.
(31) Gratzel, M.; Kalyanasundaram, K.; Thomas, J. K. *J. Am. Chem. Soc.* **1974**, *96*, 7869.
(32) Horcas, I.; et al. *Rev. Sci. Instrum.* **2007**, *78*, 013705.
(33) (a) Park, S.; Kim, B.; Wang, J. Y.; Russell, T. P. *Adv. Mater.* **2008**, *20*, 681. (b) Park, S.; Wang, J. Y.; Kim, B.; Xu, J.; Russell, T. P. *ACS Nano* **2008**, *2*, 766. (c) Park, S.; Wang, J. Y.; Kim, B.; Russell, T. P. *Nano Lett.* **2008**, *8*, 1667.
(34) Nandan, B.; Vyas, M. K.; Bohme, M.; Stamm, M. *Macromolecules* **2010**, *43*, 2463.
(35) Olszak, T. A.; Willig, F.; Durfee, W. S.; Dreissig, W.; Bradaczek, H. *Acta Crystallogr.* **1989**, *C45*, 803.
(36) Sofos, M.; Goldberger, J.; Stone, D. A.; Allen, J. E.; Ma, Q.; Herman, D. J.; Tsai, W.-W.; Lauhon, L. J.; Stupp, S. I. *Nat. Mater.* **2009**, *8*, 68.
(37) (a) Winnik, F. M. *Chem. Rev.* **1993**, *93*, 587. (b) Nakajima, A. *Bull. Chem. Soc. Jpn.* **1971**, *44*, 3272. (c) Zhang, X.; Zhang, X.; Shi, W.; Meng, X.; Lee, C.; Lee, S. *J. Phys. Chem. B* **2005**, *109*, 18777.
(38) Matsui, J.; Mitsuishi, M.; Miyashita, T. *Macromolecules* **1999**, *32*, 381.